JOURNAL OF BACTERIOLOGY, Apr. 2007, p. 3044–3050 Vol. 189, No. 8
0021-9193/07/$08.00+0 doi:10.1128/JB.01597-06

Characterization of the Proteasome Accessory Factor (*paf*) Operon in *Mycobacterium tuberculosis*▽

Richard A. Festa, Michael J. Pearce, and K. Heran Darwin*

New York University School of Medicine, Department of Microbiology, 550 First Avenue, Medical Sciences Building Room 236, New York, New York 10016

Received 13 October 2006/Accepted 29 January 2007

In a previous screen for *Mycobacterium tuberculosis* mutants that are hypersusceptible to reactive nitrogen intermediates (RNI), two genes associated with the *M. tuberculosis* proteasome were identified. One of these genes, *pafA* (*p*roteasome *a*ccessory *f*actor A), encodes a protein of unknown function. In this work, we determined that *pafA* is in an operon with two additional genes, *pafB* and *pafC*. In order to assess the contribution of these genes to RNI resistance, we isolated mutants with transposon insertions in *pafB* and *pafC*. In contrast to the *pafA* mutant, the *pafB* and *pafC* mutants were not severely sensitized to RNI, but *pafB* and *pafC* were nonetheless required for full RNI resistance. We also found that PafB and PafC interact with each other and that each is likely required for the stability of the other protein in *M. tuberculosis*. Finally, we show that the presence of PafA, but not PafB or PafC, regulates the steady-state levels of three proteasome substrates. Taken together, these data demonstrate that PafA, but not PafB or PafC, is critical for maintaining the steady-state levels of known proteasome substrates, whereas all three proteins appear to play a role in RNI resistance.

Mycobacterium tuberculosis is a successful pathogen that persists in nearly one-third of the Earth's population (11). Infection occurs by the inhalation of aerosolized droplets containing *M. tuberculosis* bacilli into the lungs, where alveolar macrophages and other phagocytic cell types then engulf the bacteria. Within these cells, *M. tuberculosis* must face various host defenses (26). One of the major protective defenses used by macrophages to contain *M. tuberculosis* infection is nitric oxide (NO), which is produced by the inducible nitric oxide synthase (19). NO and other reactive nitrogen intermediates (RNI) can damage DNA, lipids, and proteins and interfere with various cellular processes (23, 30, 36). As a result, mice that are deficient in inducible nitric oxide synthase are highly susceptible to *M. tuberculosis* infection (19). However, despite the presence of RNI, *M. tuberculosis* is able to persist within the host.

Two genes, *mpa* (*Mycobacterium p*roteasomal *A*TPase) and *pafA* (*p*roteasome *a*ccessory *f*actor), were previously identified to be important for the ability of *M. tuberculosis* to survive exposure to RNI in vitro and cause disease in vivo (6). *mpa* and *pafA* were predicted to encode proteins involved in proteasome function in bacteria (10, 22). Proteasomes are barrel-shaped proteases consisting of 14 α subunits and 14 β subunits ("20S core") (1, 18). In eukaryotes, a 19S cap complex associates with the 20S core particle. The base of the cap consists of six AAA (*A*TPase *a*ssociated with various cellular *a*ctivities) ATPases, while the lid proteins recognize ubiquitinated substrates targeted for degradation (4, 9, 25, 34). Mpa is similar to ATPases found in the eukaryotic proteasome base (7), and chemical inhibition of the *M. tuberculosis* proteasome protease activity sensitizes wild-type (WT) *M. tuberculosis* to RNI to a degree similar to that of the *mpa* or *pafA* mutants (6). The strongest evidence connecting Mpa, PafA, and the proteasome protease is the observation that all three are required for the apparent degradation of three *M. tuberculosis* proteasome substrates (24).

Although Mpa resembles proteasome-associated ATPases, PafA shares no homology with any protein of known function. In this work, we determined that *pafA* is in an operon with genes encoding two conserved proteins, Rv2096c (PafB) and Rv2095c (PafC). We also looked for interactions between proteins encoded by the *pafABC* operon and proteins involved in proteasome function. Finally, we investigated the role of each gene with respect to RNI resistance and substrate degradation by the *M. tuberculosis* proteasome. Taken together, this work represents the first study to examine the function of the previously uncharacterized *pafABC* operon.

MATERIALS AND METHODS

Bacterial strains and growth conditions. The bacterial strains used in this study are described in Table 1. *Escherichia coli* strains were grown in Luria-Bertani (LB) Miller broth (Difco) at 37°C with aeration on an orbital shaker. *E. coli* strains were chemically transformed as previously described (28). MacConkey plates with 1% maltose were prepared for use in the bacterial two-hybrid (BTH) experiments (16). For T7 promoter induction, isopropylthio-β-D-galactoside (IPTG) was added to a final concentration of 0.1 mM.

All *M. tuberculosis* strains used are derivatives of H37Rv (Table 1). *M. tuberculosis* strains were grown in Middlebrook 7H9 with ADN (0.5% bovine serum albumin [Roche], 0.2% dextrose, 0.085% sodium chloride) without shaking in 75-cm^2 vented flasks (Corning). Middlebrook 7H11 plates enriched with BBL Middlebrook oleic acid-albumin-dextrose-catalase were used to grow *M. tuberculosis* on solid media. Nitrite killing assays are described elsewhere (6).

The final concentrations of antibiotics used for *E. coli* were as follows: ampicillin, 200 μg/ml; hygromycin, 150 μg/ml; and kanamycin, 100 μg/ml. For *M. tuberculosis*, both hygromycin and kanamycin were used at a concentration of 50 μg/ml.

Plasmids. All plasmids and primers are listed in Table 1. pMV-*pafABC* was made in several cloning steps that resulted in a plasmid with a 3.5-kb fragment including 208 bp upstream of the predicted start codon of *pafA* to the stop codon of *pafC* (GenBank accession number for *pafABC*, DQ990836). pMV-*pafA* was created by digesting pMV-*pafABC* with ClaI, which deleted *pafC* and 486 bp of *pafB*. pMV-

* Corresponding author. Mailing address: New York University School of Medicine, Department of Microbiology, 550 First Avenue, Medical Sciences Building Room 236, New York, NY 10016. Phone: (212) 263-2624. Fax: (212) 263-8276. E-mail: heran.darwin@med.nyu.edu.

▽ Published ahead of print on 2 February 2007.

TABLE 1. Strains, plasmids, and primers used in this work

Strain, plasmid, or primer	Genotype or sequence	Source or reference
M. tuberculosis strains		
H37Rv	WT	ATCC 25618
MHD2	*pafA*::ΦMycoMarT7 (282)	6
MHD18	WT, pMV-306	6
MHD62	*pafA*::ΦMycoMarT7, pMV306	This work
MHD63	*pafA*::ΦMycoMarT7, pMV-*pafA*	This work
MHD64	*pafA*::ΦMycoMarT7, pMV-*pafABC*	This work
MHD75	*pafB*::ΦMycoMarT7 (769)	This work
MHD76	*pafC*::ΦMycoMarT7 (466)	This work
MHD77	*pafC*::ΦMycoMarT7 (767)	This work
MHD79	WT, pMN-FLAG-*fabD*-His_6	24
MHD78	WT, pMN-FLAG-*panB*-His_6	24
MHD82	*pafA*::ΦMycoMarT7, pMN-FLAG-*panB*-His_6	24
MHD83	*pafA*::ΦMycoMarT7, pMN-FLAG-*fabD*-His_6	24
MHD98	WT, pMV-*pafC*	This work
MHD99	*pafC*::ΦMycoMarT7 (466), pMV-*pafC*	This work
MHD100	*pafC*::ΦMycoMarT7 (767), pMV-*pafC*	This work
MHD102	*pafC*::ΦMycoMarT7 (466), pMN-FLAG-*panB*-His_6	This work
MHD112	*pafC*::ΦMycoMarT7 (466), pMN-FLAG-*fabD*-His_6	This work
MHD117	*pafB*::ΦMycoMarT7, pMN-FLAG-*fabD*-His_6	This work
MHD118	*pafB*::ΦMycoMarT7, pMN-FLAG-*panB*-His_6	This work
E. coli strains		
DH5α	F^- ϕ80d*lacZ*ΔM15 Δ(*lacZYA-argF*)*U169 deoR recA1 endA1 hsdR17* (r_K^- m_K^+) *phoA supE44* λ^- *thi-1 gyrA96 relA1*	Gibco, BRL
BTH101	F^- *cya-99 araD139 galE15 galK16 rpsL1* (Str^r) *hsdR2 mcrA1 mcrB1*	16
ER2566	F^- λ^- *fhuA2* [lon] *ompT lacZ*::*T7 geneI gal sulA11* Δ(*mcrC-mrr*)*114*::IS*10* R(*mcr-73*::miniTn10)2 R(*zgb-210*::Tn10)1 (Tet^s) *endA1* [dcm]	3
Plasmids		
pMV306	Hyg^r; integrates in single copy on the chromosome	31
pMV-*pafA*	Hyg^r; for complementation of the *pafA* mutant	This work
pMV-*pafABC*	Hyg^r; for complementation of the *pafA* mutant	This work
pMV-*pafC*	Hyg^r; for complementation of the *pafC* mutants	This work
pET24b(+)	Kan^r; for gene overexpression	Novagen
pET24b+*pafA*	Kan^r; for overexpression of *pafA*	This work
pET24b+*pafB*	Kan^r; for overexpression of *pafB*	This work
pET24b+*pafC*	Kan^r; for overexpression of *pafC*	This work
pET24b+*pafABC*	Kan^r; for overexpression of *pafABC*	This work
pUT18C*pafC*	Amp^r; *pafC* cloned into pUT18C with XbaI and KpnI, translationally fused to the C terminus of the T18 domain	This work
pUT18C*pafB*	Amp^r; *pafB* cloned into pUT18C with XbaI and KpnI, translationally fused to the C terminus of the T18 domain	This work
pKT25*pafC*	Kan^r; *pafC* cloned into pKT25 with XbaI and KpnI, translationally fused to the C terminus of the T25 domain	This work
pKT25*pafB*	Kan^r; *pafB* cloned into pKT25 with XbaI and KpnI, translationally fused to the C terminus of the T25 domain	This work
pMN-FLAG-*fabD*-His_6	Hyg^r; pMN402 with green fluorescent protein replaced by FLAG-*fabD*-His_6	24
pMN-FLAG-*panB*-His_6	Hyg^r; pMN402 with green fluorescent protein replaced by FLAG-*panB*-His_6	24
pMN-FLAG-*dlaT*-His_6	Hyg^r; pMN402 with green fluorescent protein replaced by FLAG-*dlaT*-His_6	24
pKD13	Kan^r; used for Southern analysis	8
Primers		
Rv2098c-f1	GCCTGTTCCAGGTAGGTAGT	
Rv2097c-rt	GTCATGGGTGACCAGCTGC	
Rv2098c-r1	GCCGGACGGGCCGGGGAC	
tatA-f1	GTGGGCAGTCTGAGTCCGTGGC	
tatA-rt	GCCGGCCGAGCCTCGGTGC	
Rv2095-f1	GGTCGCGTGAGGCCGAAGG	
tatC-rev1	ATGCGAATACCAGACGAACC	
pafoperon-f1	GTCACCACCGACGAAGAAAT	
pafoperon-r1	ATCCACAGCTGGTTGAGGTC	
pafB-end-BTH	GCGGTACCTCATGCCAGTGCTCCGGCTT	
pafB-start-BTH	GCTCTAGAGATGGCGACCTCGAAAGTCGAAC	
pafC-start-BTH	GCTCTAGAGATGAGCGCCCTGTCCACCCG	
pafC-end-BTH	GCGGTACCTCACGGCGGCGCAGCTGC	
pafC-rev4-HindIII	CGAAGCTTTCACGGCGGCGCAGCTGC	
pafC-rev4-HindIII-NO STOP	CGAAGCTTCGGCGGCGCAGCTGCCTGGTA	
NdeI-pafA	GGAATTCCATATGCAGCGTCGAATCATGGGC	
pafB-for1-NdeI	GGAATTCCATATGGCGACCTCGAAAGTCGAACG	
pafB-rev1-HindIII	GTCAAGCTTTGCCAGTGCTCCGGCTTGCGC	
pafC-for1-NdeI	GGAATTCCATATGAGCGCCCTGTCCACCCGG	
pafA-rev1-HindIII	GTCAAGCTTCATGCTCGCGATCAGCCGCTTAAC	
pafA-RT-for	GATCAGCCCCCACAGACC	
pafA-RT-rev	GCTTAACCCGCTCATCGAC	
pafB-RT-for	GTGTGGACCTACGCAGCAT	
pafB-RT-rev	TCGAATCTCAAGCTCGATCA	
pafC-RT-for	GCTGTTCGACGGTGACCTAT	
pafC-RT-rev	ATCCAATCCTCAGAGGCGTA	

pafC was constructed as follows: a KpnI-PstI fragment containing 208 bp upstream of the *pafA* start codon (containing the presumed native promoter) and 477 bp of *pafA* sequence was cloned upstream of a PstI-NcoI fragment containing the last 63 bp of *pafB* and the entire *pafC* coding sequence. This cloning resulted in a fusion of part of *pafA* and part of *pafB*; however, polyclonal antibodies against PafA and PafB were unable to detect this hypothetical fusion protein.

pET24b(+) was used to express *pafABC* in *E. coli* for in vitro interaction studies. pET24b+*pafABC* and pET24b+*pafABC*-His_6 were constructed using primers specific to the start of *pafA* (the GTG start site was changed to ATG for optimal expression in *E. coli*) and the end of *pafC*. pET24b+*pafABC*-His_6 does not have a stop codon, which allowed inclusion of the His_6 tag encoded in the vector. Primers included restriction sites that allowed the PCR products to be cloned into the NdeI and HindIII sites of pET24b(+).

pET24b(+) was also used for the construction of plasmids to overexpress *pafA*, *pafB*, and *pafC* individually for antibody production. These constructs were made using primers with restriction sites for NdeI and HindIII (Table 1).

All PCR-generated plasmids were sequenced by either the New York University School of Medicine DNA Sequencing Facility or Genewiz, Inc. (New Brunswick, NJ).

Mutant mining. A PCR-based approach was used to identify *pafB* and *pafC* transposon insertion mutants in a previously assembled H37Rv ΦMycoMarT7 library (6). A similar technique is described elsewhere (12, 17). The ~10,100 mutants in the library were pooled into groups of 60, and chromosomal DNA was isolated from each pool. Each pool was screened using primers specific to the *Himar* sequence of ΦMycoMarT7 (5′-AGACCGGGGACTTATCAGCCAACC TG-3′) (29) and the 3′ end of *pafC* (5′-CGCAGCTGCCTGGTATGCATCCA G-3′). Amplified products of the predicted molecular weight were gel purified and sequenced using the *Himar* primer (New York University School of Medicine DNA Sequencing Facility). Once pools with *pafB* or *pafC* mutants were identified, each mutant within a pool was separately grown in 1 ml of 7H9 plus ADN with 50 μg/ml kanamycin in 96-well plates with 2-ml wells (Nunc). After 2 weeks, chromosomal DNA was purified from individual mutants (Ultra Clean DNA purification kit; MoBio), and PCR was used as described above to identify mutants within the pool. Once identified, each mutant was single-colony purified by passing a mid- to late-log-phase culture through a 5.0-μm filter (Millipore) by gravity flow. The resulting cell suspension was inoculated onto solid medium and incubated for 2 to 3 weeks. The presence of a single transposon insertion in each mutant was confirmed by Southern blotting. Genomic DNA was digested with BamHI and transferred to a nylon membrane (Hybond-XL; Amersham Biosciences). To probe for the presence of the transposon insertion on the chromosome, we used the entire pKD13 plasmid digested with HindIII to probe for the neomycin (kanamycin resistance) cassette encoded on the transposon. Detection was performed using the DIG High Prime DNA labeling and detection starter kit I (Roche).

RNA isolation, reverse transcriptase PCR (RT-PCR), and qRT-PCR. RNA was extracted from *M. tuberculosis* cultures grown in 7H9 plus ADN to an optical density at 580 nm (OD_{580}) of 1.0. An equal volume of 4 M guanidinium isothiocyanate–0.5% sodium *N*-lauryl sarcosine–25 mM trisodium citrate was added to cultures to arrest transcription, and cells were pelleted at 2,885 × *g*. Bacterial pellets were resuspended in 1 ml TRIzol reagent (Invitrogen) and bead beaten with zirconia silica beads (BioSpec Products) in a BioSpec Mini Bead Beater two times for 30 s, with cooling of the samples on ice in between. Preparation of the RNA was performed as described by the manufacturer. RNA extraction was repeated two more times to ensure removal of all genomic DNA. RNA was stored in aliquots at −80°C. cDNA was synthesized using the Reverse Transcriptase System (Promega) with 100 ng of total *M. tuberculosis* RNA and random hexamers (Amersham Biosciences). For quantitative real-time PCR (qRT-PCR), we used Platinum SYBR green PCR SuperMix UDG (Invitrogen) in a Bio-Rad MyiQ real-time PCR system.

BTH analysis. BTH assays were performed as described previously (16). Protein fusions were constructed using pUT18C or pKT25 plasmids, and the primers used to make fusions in this study are listed in Table 1. BTH101 cells were transformed with both plasmids and inoculated onto MacConkey agar supplemented with 1% maltose. Colonies were colony purified on the same medium. β-Galactosidase assays were performed as previously described to quantify the interactions between two fusion proteins (21).

Affinity chromatography. Plasmids used for the production of His_6-tagged Paf proteins are listed in Table 1. One-hundred-milliliter cultures of *E. coli* strains containing plasmids carrying *pafABC* or *pafABC*-His_6 were induced with IPTG at an OD_{600} of 0.6 for 5 h at 26°C. Cell lysates were prepared exactly as described in The QIAexpressionist manual. To examine protein-protein interactions, proteins were purified under native conditions. Lysate (750 μl) was then added to 30 μl of Ni-nitrilotriacetic acid (Ni-NTA) agarose (QIAGEN) and incubated with agitation for 1 h at 4°C. Ni-NTA agarose was pelleted and washed with 750 μl wash buffer (50 mM NaH_2PO_4, 300 mM NaCl, 20 mM imidazole) three times. The agarose was resuspended in 200 μl of elution buffer (50 mM NaH_2PO_4, 300 mM NaCl, 250 mM imidazole) and collected by centrifugation, and the supernatant was saved ("elution"). This was repeated four times to obtain four elutions. Samples were boiled for 5 min, and PafA, PafB, and PafC were detected by immunoblotting.

Antibodies and immunoblotting. Purification of proteins for antibody production was performed under denaturing conditions according to the manufacturer's specifications (QIAGEN). Polyclonal rabbit antibodies were raised against PafA, PafB, and PafC with C-terminal His_6 tags, each expressed individually in *E. coli*. Antibodies were produced using Freund's incomplete adjuvant by Sigma-Genosys (St. Louis, MO). Mpa and DlaT antibodies were described previously (7, 32). For immunoblotting analysis, cell numbers equivalent to 10 OD_{580} units were harvested. Bacteria were washed once in an equal volume of phosphate-buffered saline–0.05% Tween 20 and were resuspended in 350 μl of lysis buffer (100 mM Tris-Cl, 100 mM KCl, 1 mM EDTA, 5 mM $MgCl_2$, pH 8). Cells were lysed by bead beating with zirconia beads three times for 30 s. Total cell lysate (150 μl) was mixed with 50 μl of 4× sodium dodecyl sulfate sample buffer and boiled for 10 min. Immunoblotting was performed as previously described (14). Antibodies to His_6-tagged PafA, PafB, and PafC antibodies were affinity purified as described elsewhere (7). Anti-PafA was used at a dilution of 1:1,000, and antibodies to PafB and PafC were used at a dilution of 1:100. FLAG antibodies were purchased from Sigma (St. Louis, MO). Horseradish peroxidase-conjugated goat anti-rabbit antibodies (Amersham Biosciences) were used for chemiluminescent detection (SuperSignal West Pico or Femto chemiluminescent substrate; Pierce). Antibodies to DlaT (dihydrolipoamide acyltransferase) were a kind gift from Ruslana Bryk and Carl Nathan.

RESULTS

Complementation of the *pafA* transposon mutation. *pafA* transposon mutants are severely sensitive to RNI in vitro (6). We attempted to complement the *pafA* transposon mutation by introducing *pafA* in single copy into the *M. tuberculosis* chromosome at the *attB* site. When exposed to 3 mM sodium nitrite in medium at pH 5.5 for 6 days, the *pafA* mutation was partially complemented for the RNI-sensitive phenotype (Fig. 1A). To determine if the entire *pafABC* operon could fully complement the *pafA* mutation, we introduced pMV-*pafABC* into the *pafA* mutant. Survival after RNI treatment was restored to WT levels (Fig. 1A). These data suggested that the sensitivity to RNI of the *pafA* mutant was partly due to the polarity of this mutation on *pafB* and/or *pafC*. Consistent with this hypothesis, PafB and PafC proteins were undetectable in the *pafA* mutant (Fig. 1B). Furthermore, RT-PCR revealed that there was no *pafB* or *pafC* transcript in the *pafA* mutant (data not shown). Thus, the *pafA* transposon mutation was polar on *pafBC* expression.

Examination of the DNA sequence around *pafA* suggested that *pafA* forms an operon with the two downstream genes, *pafB* and *pafC*. In *M. tuberculosis*, *pafA* and *pafB* are separated by eight nucleotides, while the stop codon of *pafB* overlaps the *pafC* start codon. The *pafABC* operon structure is conserved, and the predicted gene products are homologous only between other *Actinomycetales* (Fig. 2A). At 65 bp downstream of *pafC* is *tatA*, which is involved in the twin-arginine translocation (Tat) pathway. The Tat pathway translocates folded proteins across the cell membranes in numerous gram-positive and gram-negative bacteria (2), as well as in *Mycobacterium smegmatis* (20). This gene is not always located downstream of the *pafABC* operon in other *Actinomycetales*. Rv2098c is 52 base pairs upstream of the predicted start codon of *pafA* and encodes a hypothetical protein, PE_PGRS36, which contains a frameshift mutation towards the 5′ region of the open reading

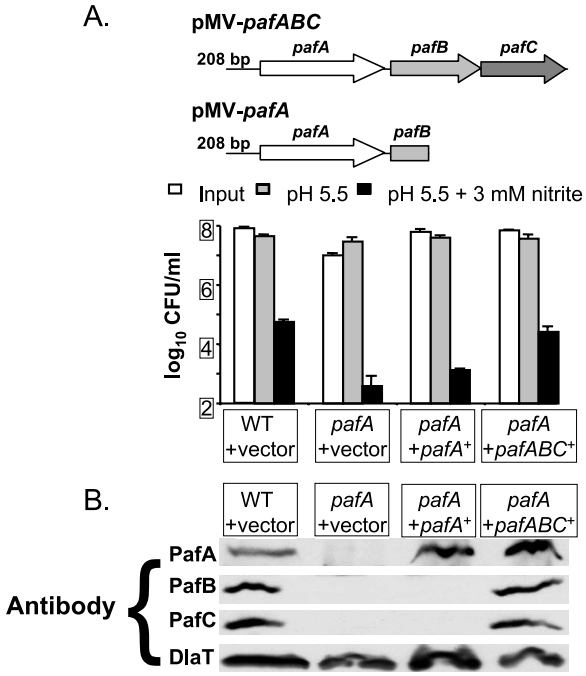

FIG. 1. Complementation of a *pafA* transposon mutation. (A) Top, schematic of the pMV-*pafABC* and pMV-*pafA* complementation plasmids. Bottom, assay for *M. tuberculosis* RNI resistance in vitro, showing CFU/ml of WT *M. tuberculosis* containing pMV306 (vector), the *pafA* mutant with pMV306, and the *pafA* mutant with pMV-*pafA* or pMV-*pafABC* after exposure to acidified medium (pH 5.5) (gray bars) or acidified medium with 3 mM nitrite (black bars) for 6 days. White bars indicate starting CFU/ml. One experiment representative of three independent experiments, each done in triplicate, is shown. Error bars indicate standard deviations. (B) Immunoblot analysis of PafA, PafB, and PafC in total cell lysates without exposure to RNI. DlaT (dihydrolipoamide acyltransferase) was used as a loading control.

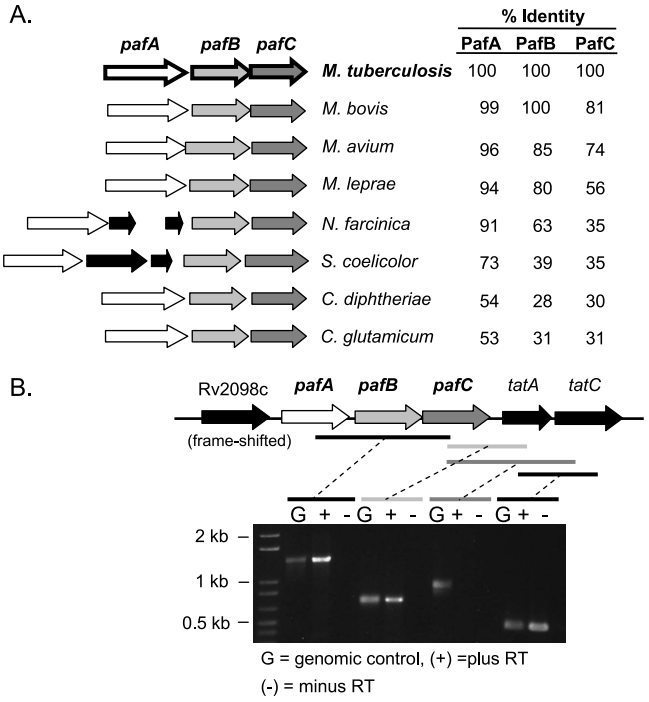

FIG. 2. Organization of the *pafABC* operon in the *Actinomycetales*. (A) Schematic showing the organization of the *pafABC* operon in selected *Actinomycetales*. The percent identity of each protein orthologue to the *M. tuberculosis* protein is noted. Between *pafA* and *pafB*, *Nocardia farcinica* encodes a hypothetical protein and a putative transcriptional regulator and *Streptomyces coelicolor* encodes a peptidyl-prolyl *cis-trans* isomerase (*fkb*) and a hypothetical protein. (B) PCR analysis of cDNA made from WT *M. tuberculosis* RNA. The genetic organization of this region is shown above. Black and gray bars indicate the amplified regions.

frame. An Rv2098c transcript was not detected by RT-PCR (data not shown). Additionally, it does not appear that Rv2098c is cotranscribed with *pafA*, because we could not detect a transcript between Rv2098c and *pafA* (data not shown).

Our complementation data suggested that the *pafA* mutation was polar on the expression of *pafB* and *pafC*, based on the absence of *pafBC* message and PafB and PafC proteins in the *pafA* mutant. We performed RT-PCR analysis to determine if *pafABC* was transcribed as a single message. Primers spanning from the middle of *pafA* to the middle of *pafC* amplified an approximately 1.4-kb product (Fig. 2B). DNA sequence analysis of this product confirmed that *pafA*, *pafB*, and *pafC* are indeed cotranscribed in WT *M. tuberculosis*. In addition, it appeared that *tatA*, which is predicted to be essential (29), is cotranscribed with *pafC* (Fig. 2B). In contrast, *tatC*, which is immediately downstream of *tatA*, does not appear to be cotranscribed with *pafC*. However, *tatC* is cotranscribed with *tatA* (Fig. 2B) (27). Therefore, it appears that there is readthrough transcription from the *pafA* operon to *tatA*, as well as expression of *tatAC* from a *tat*-specific promoter. qRT-PCR showed no change in *tatA* transcript levels between WT *M. tuberculosis* and the *pafA* transposon mutant strains (data not shown), suggesting that the *pafC-tatA* readthrough transcript is a minor product. Importantly, *tatA* does not appear to affect RNI resistance in the *pafA* transposon mutant, as *pafABC* was sufficient to restore RNI resistance to the *pafA* mutant.

***pafB* and *pafC* mutants have a subtle RNI-sensitive phenotype.** *pafB* and *pafC* in addition to *pafA* are required to fully complement the *pafA* mutation, so we wanted to determine the individual contributions of these genes to RNI sensitivity. We isolated *pafB* and *pafC* mutants from a library of 10,100 transposon mutants (6). We identified mutants with transposon insertions at nucleotide 769 of *pafB* and at nucleotides 466 and 767 of *pafC*.

The *pafB* and *pafC* mutants were tested for sensitivity to RNI. Neither mutant was as susceptible to RNI as the *pafA* mutant; however, the *pafB* and *pafC* mutants were more susceptible than WT *M. tuberculosis* to RNI-induced killing (Fig. 3A). The *pafB* and *pafC* mutants were consistently killed between 5- and 65-fold more than WT *M. tuberculosis*; however, the statistical significance of these results varied across experiments (not shown). Figure 3A represents one experiment where the difference in the degree of RNI-induced killing between the WT and the *pafB* or *pafC* mutants had a *P* value of ≤ 0.05. Compared to the *pafA* mutant ($P < 0.004$), these mutants had a much more subtle phenotype. This likely explains why we did not identify the *pafB* and *pafC* mutants, which were present in the screened library, in the previous

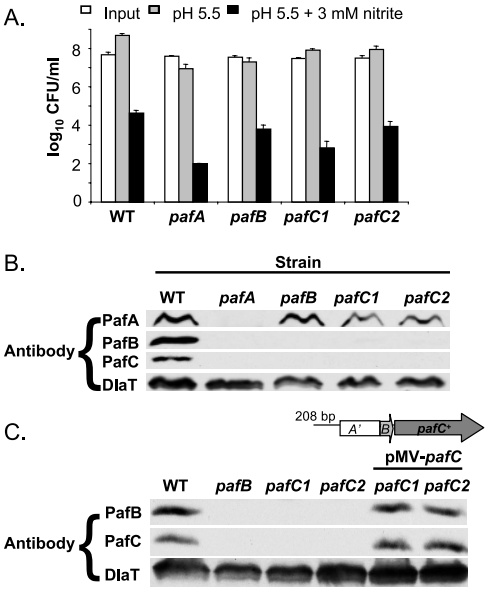

FIG. 3. *pafB* and *pafC* mutants are susceptible to RNI. (A) RNI survival assay, as described for Fig. 1A, of a *pafB* mutant and two *pafC* mutants. This experiment represents one of three independent experiments, each done in triplicate. Error bars indicate standard deviations. (B) Total cell lysates of WT, *pafA*, *pafB*, and two *pafC* strains were tested for the presence of PafA, PafB, PafC, and DlaT by immunoblotting. (C) Detection of PafB and PafC in WT, *pafB*, *pafC*, and *pafC*-complemented strains. Antibodies against DlaT were used for the loading control. A schematic of the pMV-*pafB* complementation plasmid is also shown.

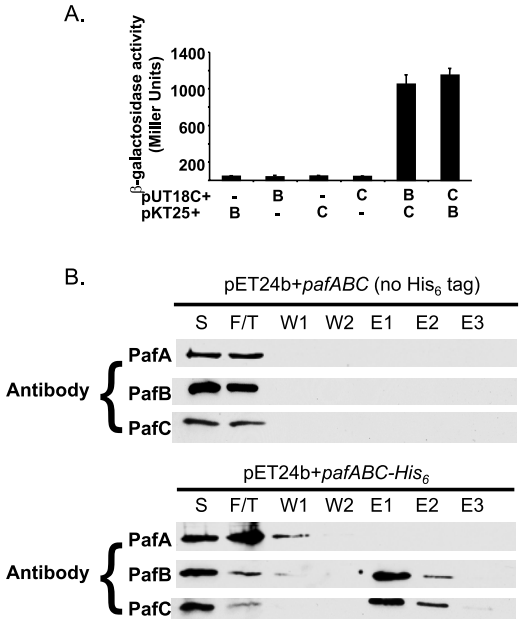

FIG. 4. PafB and PafC interact. (A) BTH interactions were quantified by β-galactosidase assay. Constructs used are denoted beneath the bars, where *pafB* ("B") or *pafC* ("C") was fused to the T18 or T25 domain of Cya in pUT18C or pKT25, respectively. Each assay was done in triplicate using three independent samples per assay that were then averaged. These results are representative of two independent experiments. Error bars indicate standard deviations. (B) PafB co-elutes with PafC-His_6 from nickel-agarose. Immunoblot analysis was performed on the soluble lysates ("S"), flowthrough ("F/T"), two washes ("W"), and the first three elutions ("E") using polyclonal antibodies to PafA, PafB, and PafC. Paf proteins were not detected in the fourth elution (not shown).

screen for RNI-sensitive mutants (6). Nonetheless, these data showed for the first time that *pafB* and *pafC* were playing at least a small role in resistance to RNI in vitro.

We examined Paf protein levels in the *pafB* and *pafC* mutants. Although PafA was present at similar levels in the *pafB* and *pafC* mutants, both PafB and PafC were absent from either the *pafB* or *pafC* mutants (Fig. 3B). We checked for the presence of *pafB* or *pafC* mRNA in the *pafC* or *pafB* mutant, respectively, using RT-PCR and found that *pafB* mRNA was present in the *pafC* mutant and that *pafC* mRNA was present in the *pafB* mutant (data not shown). Because PafB and PafC were both absent in either the *pafB* or the *pafC* mutant, despite the presence of the respective mRNA, we hypothesized that each protein was necessary for the stability of the other. To test this, we complemented the *pafB* mutation with pMV-*pafB* and the *pafC* mutation by using pMV-*pafC*. Complementation of the *pafB* mutation with *pafB* did not restore steady-state PafC protein levels, despite restoring PafB protein levels (data not shown). This was not surprising, because the transposon insertion that introduced at least one stop codon in *pafB* most likely uncoupled translation from transcription of *pafC*. In addition, although we could qualitatively observe *pafC* transcript in the *pafB* mutant, it is possible that the *pafC* transcript was less abundant than in WT *M. tuberculosis*, further reducing PafC protein levels. Although PafB protein could be restored in the absence of PafC, this may be due to increased expression or translation of *pafB* expressed from the complementation plasmid.

In contrast to the case for the *pafB* insertion mutation, we found that complementation of the *pafC* mutation restored WT levels of both PafB and PafC (Fig. 3C). This suggested that PafC was required for the stability of PafB (Fig. 3C) and supported the hypothesis that PafB and PafC could interact.

PafB and PafC interact. PafB levels were affected by the absence of PafC; therefore, we hypothesized that these two proteins interacted with each other. We used a BTH approach to look for the interactions between PafB and PafC. This assay utilizes two domains of the adenylate cyclase from *Bordetella pertussis* (T25 and T18), each encoded on a separate plasmid (16). These plasmids are introduced into an adenylate cyclase (*cya*) mutant of *E. coli* that cannot use several carbon sources, including maltose and lactose. If two proteins of interest interact, they will bring the two Cya domains together, resulting in the production of cyclic AMP. This complements the *cya* mutation and allows the metabolism of maltose or lactose, which can be quantified by β-galactosidase assays. BTH analysis revealed that PafB and PafC interact strongly (Fig. 4A). This result was comparable to those for previously tested interactions between other proteasome-associated components (i.e., PrcA with PrcB and Mpa with Mpa) with well-established interactions (6, 7, 15). Neither fusion measured β-galactosidase activity above background with any other proteins tested, including PafA, Mpa, and PrcA (the α subunit of the *M. tuberculosis* proteasome) (data not shown). However, this does not rule out possible interactions with these or other proteins;

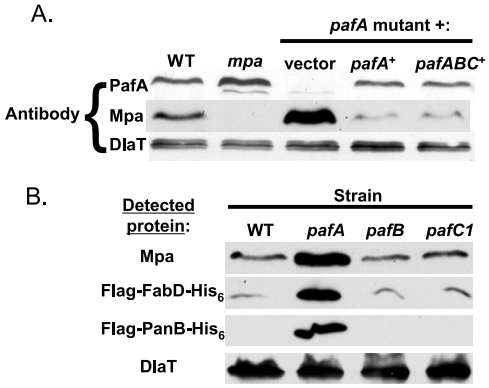

FIG. 5. PafA, but not PafB or PafC, is required for maintaining WT steady-state levels of *M. tuberculosis* proteasome substrates. (A) Immunoblot analysis of Mpa in the WT and a *pafA* mutant complemented with empty vector and in the *pafA* mutant with pMV-*pafA* or pMV-*pafABC*. (B) Immunoblot analysis of Mpa, FLAG-FabD-His_6, and FLAG-PanB-His_6 in WT, *pafA*, *pafB*, and *pafC* strains. Proteins were detected using antibodies to Mpa or the FLAG epitope. Antibodies to DlaT were used for the loading control.

for example, the Cya domains may sterically hinder some protein-protein interactions.

The interaction observed between PafB and PafC in the BTH system was validated using Ni-NTA affinity chromatography. PafA, PafB, and PafC were produced in *E. coli* by using two *pafABC* constructs: one with a C-terminal His_6 epitope tag encoded at the end of *pafC* and the other without a His_6 tag. After incubation of lysates made from these strains with Ni-NTA beads and subsequent washing, immunoblot analysis of the eluted proteins showed that PafB specifically eluted with PafC-His_6 (Fig. 4B). PafA did not elute with PafBC but was found in the flowthrough and wash fractions (Fig. 4B). Importantly, PafB did not bind to the Ni-NTA agarose nonspecifically (Fig. 4B). Taken together, these data show that PafB and PafC interact, and this interaction may explain why PafC is necessary for the steady-state stability of PafB in *M. tuberculosis*.

Mutations in *pafB and pafC* do not affect the stability of proteasome substrates in *M. tuberculosis*. We recently determined that Mpa and PafA are required for the apparent degradation of three proteins: FabD (malonyl coenzyme A acyl carrier protein transacylase), PanB (ketopantoate hydroxymethyltransferase), and Mpa itself (24). In this work, we show that there is no PafB or PafC in the *pafA* mutant; thus, it was possible that PafB and PafC were also important for the stability of these proteins. Immunoblot analysis of total *M. tuberculosis* cell lysates showed that Mpa levels were dramatically increased in the *pafA* mutant compared to WT *M. tuberculosis* (Fig. 5A) (24). Complementation of the *pafA* mutation with *pafA* or *pafABC* restored Mpa to WT levels (Fig. 5A). In contrast to the case for the *pafA* mutant, Mpa levels appeared similar to those seen in WT *M. tuberculosis* in both the *pafB* and *pafC* mutants, suggesting that PafB and PafC do not regulate Mpa levels (Fig. 5B).

We then examined the steady-state levels of FabD and PanB in the *pafB* and *pafC* mutants. FLAG-*fabD*-His_6 and FLAG-*panB*-His_6 were expressed in *M. tuberculosis* under the control of a heterologous mycobacterial *hsp60* promoter and an *E. coli* ribosome-binding site (24). In contrast to the *mpa* and *pafA* mutants (24), epitope-tagged FabD and PanB did not accumulate in the *pafB* and *pafC* mutants (Fig. 5B; data not shown for *pafC2*). Thus, these data suggest that PafB and PafC are not necessary for the degradation of these substrates by the *M. tuberculosis* proteasome under the conditions tested.

DISCUSSION

This work has furthered our understanding of the previously uncharacterized *pafABC* operon. We have determined that *pafA* is cotranscribed with two additional genes, *pafB* and *pafC*. We showed that the RNI-sensitive phenotype caused by the transposon insertion in *pafA* was due to a lack of expression of the *pafABC* operon and not just *pafA*. While these data suggested that *pafB* and *pafC* have a role in RNI resistance, *pafB* and *pafC* transposon mutants were not as sensitive to RNI as *pafA* mutants. Our work also demonstrated that PafB and PafC interact, suggesting that PafB-PafC complex formation is required for their function. Finally, we showed that presumptive proteasome substrates did not accumulate in the *pafB* or *pafC* mutants, suggesting that PafB and PafC do not play as important a role in proteasome function as PafA and Mpa.

The *pafABC* operon is conserved in several other *Actinomycetales*. When comparing this operon to other species in the genus *Mycobacterium*, PafA is the most highly conserved protein, with >94% identity, while PafB and PafC are not as conserved (Fig. 2A). Interestingly, *Mycobacterium leprae*, the obligate host-associated bacterium that causes leprosy, maintains an intact *pafABC* operon despite having undergone massive genome decay (5, 33). *pafA* and the proteasome protease genes (*prcBA*) are expressed in *M. leprae* based on microarray analysis (Ric Slayden and Diana Williams, personal communication) (35). If *M. leprae* has conserved a minimal number of genes necessary for survival in vivo, this suggests that the *paf* operon plays an integral role during infection.

Outside of the genus *Mycobacterium*, the homology between PafB or PafC and its orthologues sharply declines, perhaps suggesting a less important role for these proteins than for PafA. Representative species from the genera *Nocardia* and *Streptomyces* are exceptional in that they contain genes in between *pafA* and *pafB* (Fig. 2A). However, these genes appear to be unrelated to the *paf* genes as well as to each other. *Corynebacterium* species do not appear to encode proteasome protease subunits, perhaps explaining why the PafABC proteins are the most degenerate compared to the other species. It is possible that the functions of these proteins are used differently in *Corynebacterium* species or are involved with another protease system.

Currently, very little is known about proteasome biology in prokaryotes. In the eukaryotic proteasome system, the 19S complex that associates with the proteasome core consists roughly of two parts, the base, which binds to the protease core, and the lid (34). This 19S complex consists of six ATPases as well as non-ATPase subunits (34). Due to the lack of ubiquitin and homologous 19S cap structures in bacteria, it is likely that the *M. tuberculosis* proteasome uses a different system for targeting proteins for degradation. PafA appears to be required for protein degradation by the *M. tuberculosis* protea-

some (Fig. 5B) (24), perhaps having a function similar to that of the non-ATPase subunits of the eukaryotic 19S regulatory complex. This may include the binding and recognition of substrates targeted for proteolysis.

Although PafB and PafC do not appear to be required for the degradation of known substrates, it is possible that they are involved in the degradation of other, unidentified substrates. There is precedence for the presence of different "adaptor" requirements for protein degradation. For example, the sigma factor RpoS, but not the lambda O protein, requires RssB for degradation by ClpXP in *E. coli* (37). Other adaptors have been found to be involved in selectively targeting proteins to proteases in both gram-negative and gram-positive bacteria (13). Clp proteases are biochemically different from the proteasome, but the idea that proteins are selectively degraded by different targeting mechanisms is likely to be a conserved theme. Future studies will test this hypothesis. Importantly, these studies will be critical as we design experiments to reconstitute proteasome activity in vitro. This work shows that PafA is an integral part of protein degradation by the proteasome, whereas PafB and PafC appear to be less important for proteasome function under the conditions tested.

ACKNOWLEDGMENTS

We thank Susan Butler-Wu, Andrew Darwin, Catherine Potenski, and Naoko Tanese for critically reviewing the manuscript. We thank Diana Williams and Ric Slayden for sharing unpublished results.

M.J.P. was supported by grant 5T32 AI07189-25. This work was supported by a Center for AIDS Research (CFAR) Pilot Project grant (NIH S P30 A1027742-17) awarded to K.H.D.

REFERENCES

1. **Baumeister, W., J. Walz, F. Zühl, and E. Seemüller.** 1998. The proteasome: paradigm of a self-compartmentalizing protease. Cell **92:**367–380.
2. **Berks, B. C., T. Palmer, and F. Sargent.** 2005. Protein targeting by the bacterial twin-arginine translocation (Tat) pathway. Curr. Opin. Microbiol. **8:**174–181.
3. **Chong, S., and G. A. Garcia.** 1994. A versatile and general prokaryotic expression vector, pLACT7. BioTechniques **17:**686, 688, 690–691.
4. **Chu-Ping, M., J. H. Vu, R. J. Proske, C. A. Slaughter, and G. N. DeMartino.** 1994. Identification, purification, and characterization of a high molecular weight, ATP-dependent activator (PA700) of the 20 S proteasome. J. Biol. Chem. **269:**3539–3547.
5. **Cole, S. T., K. Eiglmeier, J. Parkhill, K. D. James, N. R. Thomson, P. R. Wheeler, N. Honoré, T. Garnier, C. Churcher, D. Harris, K. Mungall, D. Basham, D. Brown, T. Chillingworth, R. Conner, R. M. Davies, K. Devlin, K. Duthoy, T. Feltwell, A. Fraser, N. Hamlin, S. Holroyd, T. Hornsby, K. Jagels, C. Lacroix, J. Mclean, S. Moule, L. Murphy, K. Oliver, M. A. Quail, M.-A. Rajandream, K. M. Rutherford, S. Rutter, K. Seeger, S. Simon, M. Simmonds, J. Skelton, R. Squares, S. Squares, K. Stevens, K. Taylor, S. Whitehead, J. R. Woodward, and B. G. Barrell.** 2001. Massive gene decay in the leprosy bacillus. Science **409:**1007–1011.
6. **Darwin, K. H., S. Ehrt, N. Weich, J.-C. Gutierrez-Ramos, and C. F. Nathan.** 2003. The proteasome of Mycobacterium tuberculosis is required for resistance to nitric oxide. Science **302:**1963–1966.
7. **Darwin, K. H., G. Lin, Z. Chen, H. Li, and C. Nathan.** 2005. Characterization of a Mycobacterium tuberculosis proteasomal ATPase homologue. Mol. Microbiol. **55:**561–571.
8. **Datsenko, K. A., and B. L. Wanner.** 2000. One-step inactivation of chromosomal genes in Escherichia coli K-12 using PCR products. Proc. Natl. Acad. Sci. USA **97:**6640–6645.
9. **DeMartino, G. N., C. R. Moomaw, O. P. Zagnitko, R. J. Proske, M. Chu-Ping, S. J. Afendis, J. C. Swaffield, and C. A. Slaughter.** 1994. PA700, an ATP-dependent activator of the 20 S proteasome, is an ATPase containing multiple members of a nucleotide-binding protein family. J. Biol. Chem. **269:**20878–20884.
10. **De Mot, R., I. Nagy, J. Walz, and W. Baumeister.** 1999. Proteasomes and other self-compartmentalizing proteases in prokaryotes. Trends Microbiol. **7:**88–92.
11. **Dye, C., S. Scheele, P. Dolin, V. Pathania, M. C. Raviglione, et al.** 1999. Global burden of tuberculosis: estimated incidence, prevalence, and mortality by country. JAMA. **282:**677–686.
12. **Ewann, F., M. Jackson, K. Pethe, A. Cooper, N. Mielcarek, D. Ensergueix, B. Gicquel, C. Locht, and P. Supply.** 2002. Transient requirement of the PrrA-PrrB two-component system for early intracellular multiplication of *Mycobacterium tuberculosis*. Infect. Immun. **70:**2256–2263.
13. **Gottesman, S.** 2003. Proteolysis in bacterial regulatory circuits. Annu. Rev. Cell Dev. Biol. **19:**565–587.
14. **Harlow, E., and D. P. Lane.** 1988. Antibodies: a laboratory manual. Cold Spring Harbor Laboratory Press, Cold Spring Harbor, NY.
15. **Hu, G., G. Lin, M. Wang, L. Dick, R.-M. Xu, C. Nathan, and H. Li.** 2006. Structure of the Mycobacterium tuberculosis proteasome and mechanism of inhibition by a peptidyl boronate. Mol. Microbiol. **59:**1417–1428.
16. **Karimova, G., A. Ullmann, and D. Ladant.** 2000. A bacterial two-hybrid system that exploits a cAMP signaling cascade in Escherichia coli. Methods Enzymol. **328:**59–73.
17. **Lane, J. M., and E. J. Rubin.** 2006. Scaling down: a PCR-based method to efficiently screen for desired knockouts in a high density Mycobacterium tuberculosis picked mutant library. Tuberculosis **86:**310–313.
18. **Lin, G., G. Hu, C. Tsu, Y. Z. Kunes, H. Li, L. Dick, T. Parsons, P. Li, Z. Chen, P. Zwickl, N. Weich, and C. Nathan.** 2006. Mycobacterium tuberculosis prcBA genes encode a gated proteasome. Mol. Microbiol. **59:**1405–1416.
19. **MacMicking, J. D., R. J. North, R. LaCourse, J. S. Mudgett, S. K. Shah, and C. F. Nathan.** 1997. Identification of nitric oxide synthase as a protective locus against tuberculosis. Proc. Natl. Acad. Sci. USA **94:**5243–5248.
20. **McDonough, J. A., K. E. Hacker, A. R. Flores, M. S. Pavelka, Jr., and M. Braunstein.** 2005. The twin-arginine translocation pathway of *Mycobacterium smegmatis* is functional and required for the export of mycobacterial beta-lactamases. J. Bacteriol. **187:**7667–7679.
21. **Miller, J. H.** 1972. Experiments in molecular genetics. Cold Spring Harbor Laboratory, Cold Spring Harbor, NY.
22. **Nagy, I., S. Geert, J. Vanderleyden, and R. De Mot.** 1997. Further sequence analysis of the DNA regions with the *Rhodococcus* 20S proteasome structural genes reveals extensive homolgy with *Mycobacterium leprae*. DNA Seq. **7:**225–228.
23. **Nathan, C. F., and M. U. Shiloh.** 2000. Reactive oxygen and nitrogen intermediates in the relationship between mammalian hosts and microbial pathogens. Proc. Natl. Acad. Sci. USA **97:**8841–8848.
24. **Pearce, M. J., P. Arora, R. A. Festa, S. M. Butler-Wu, R. S. Gokhale, and K. H. Darwin.** 2006. Identification of substrates of the Mycobacterium tuberculosis proteasome. EMBO J. **25:**5423–5432.
25. **Pickart, C. M., and R. E. Cohen.** 2004. Proteasomes and their kin: proteases in the machine age. Nat. Rev. Mol. Cell. Biol. **5:**177–187.
26. **Russell, D. R.** 2001. Mycobacterium tuberculosis: here today, and here tomorrow. Nat. Rev. **2:**1–9.
27. **Saint-Joanis, B., C. Demangel, M. Jackson, P. Brodin, L. Marsollier, H. Boshoff, and S. T. Cole.** 2006. Inactivation of Rv2525c, a substrate of the twin-arginine translocation (Tat) system of *Mycobacterium tuberculosis*, increases beta-lactam susceptibility and virulence. J. Bacteriol. **188:**6669–6679.
28. **Sambrook, J., T. Maniatis, and E. Fritsch.** 1989. Molecular cloning: a laboratory manual. Cold Spring Harbor Laboratory Press, Cold Spring Harbor, NY.
29. **Sassetti, C. M., D. H. Boyd, and E. J. Rubin.** 2001. Comprehensive identification of conditionally essential genes in mycobacteria. Proc. Natl. Acad. Sci. USA **98:**12712–12717.
30. **Shiloh, M. U., and C. F. Nathan.** 2000. Reactive nitrogen intermediates and the pathogenesis of Salmonella and mycobacteria. Curr. Opin. Microbiol. **3:**35–42.
31. **Stover, C. K., V. F. de la Cruz, T. R. Fuerst, J. E. Burlein, L. A. Benson, L. T. Bennett, G. P. Bansal, J. F. Young, M. H. Lee, G. F. Hatfull, et al.** 1991. New use of BCG for recombinant vaccines. Nature **351:**456–460.
32. **Tian, J., R. Bryk, M. Itoh, M. Suematsu, and C. Nathan.** 2005. Variant tricarboxylic acid cycle in Mycobacterium tuberculosis: identification of alpha-ketoglutarate decarboxylase. Proc. Natl. Acad. Sci. USA **102:**10670–10675.
33. **Vissa, V. D., and P. J. Brennan.** 2001. The genome of Mycobacterium leprae: a minimal mycobacterial gene set. Genome Biol. **2:**REVIEWS1023.
34. **Voges, D., P. Zwickl, and W. Baumeister.** 1999. The 26S proteasome: a molecular machine designed for controlled proteolysis. Annu. Rev. Biochem. **68:**1015–1068.
35. **Williams, D. L., M. Torrero, P. R. Wheeler, R. W. Truman, M. Yoder, N. Morrison, W. R. Bishai, and T. P. Gillis.** 2004. Biological implications of Mycobacterium leprae gene expression during infection. J. Mol. Microbiol. Biotechnol. **8:**58–72.
36. **Zahrt, T. C., and V. Deretic.** 2002. Reactive nitrogen and oxygen intermediates and bacterial defenses: unusual adaptations in Mycobacterium tuberculosis. Antioxid. Redox Signal. **4:**141–159.
37. **Zhou, Y., and S. Gottesman.** 1998. Regulation of proteolysis of the stationary-phase sigma factor RpoS. J. Bacteriol. **180:**1154–1158.